Gaikwad *et al.*
Future Journal of Pharmaceutical Sciences (2023) 9:43
https://doi.org/10.1186/s43094-023-00494-0

Future Journal of Pharmaceutical Sciences

RESEARCH Open Access

Design, development, and evaluation of docetaxel-loaded niosomes for the treatment of breast cancer

Dipika S. Gaikwad[1], Rutuja D. Chougale[1,2], Kiran S. Patil[1,2*], John I. Disouza[3] and Ashok A. Hajare[2]

Abstract

Background Docetaxel (DTX) has been used to treat numerous types of cancers. Poor solubility, lower bioavailability, and serious side effects limit its use in cancer treatment. The objective of the present research work was to develop DTX-loaded niosomes to overcome these issues and investigate the anticancer effect on breast cancer. Niosomes of DTX were prepared and evaluated to estimate particle size, surface potential, morphology by TEM, %EE, in vitro drug release, %hemolysis, in vitro cytotoxicity, and stability. The cytotoxicity effect of plain DTX and DTX-loaded niosomes was performed on MCF-7 cell lines.

Results The mean particle size, zeta potential, and %EE of DTX-loaded niosomes were 244.9 nm, − 7.1 mV, and 97.43%, respectively. Besides, combining the DTX with polymers enhanced drug loading capacity. The TEM images confirmed spherical-shaped niosomes. The IR, DSC, and P-XRD studies indicate no chemical interaction between drug and excipients. The developed DTX niosomes showed a sustained release behavior and lower in vitro cytotoxicity when compared to plain DTX.

Conclusion The current research work demonstrates the suitability of co-loading of DTX in niosomes as a promising approach to enhance the efficiency of DTX.

Keywords Docetaxel, Niosomes, 3^2 factorial design, In vitro cytotoxicity

*Correspondence:
Kiran S. Patil
kspatil.tkcp@gmail.com
Full list of author information is available at the end of the article

Graphical Abstract

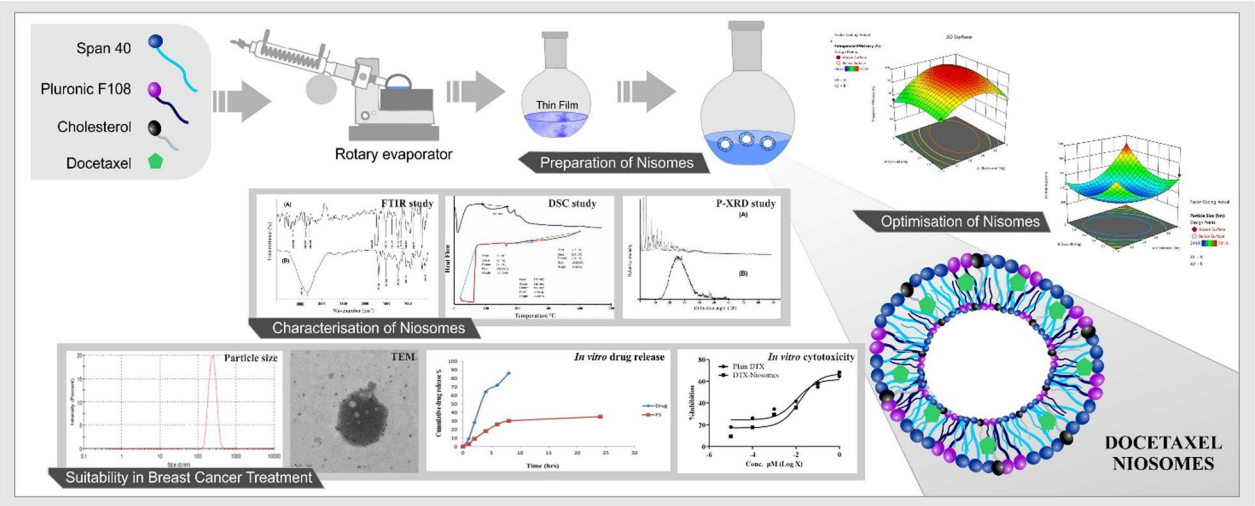

Background

Today globally, breast cancer is the most common type of cancer with 12% of all new annual cancer cases worldwide. The World Health Organization (WHO) has estimated that about 30% of newly diagnosed cases of cancers in women will be breast cancers [1]. Globally, cancer is a leading cause of death and a significant obstacle to raising life expectancy [2]. Cancer is the uncontrolled cell division that spreads abnormally growing cells across other organs, interfering with normal organ function and, in some cases, leading to death [3]. The development of tumors in cancer is the net result of the uncontrolled division of abnormal cells that affects the body [4]. In cancer patients, normal cell function is lost during the penetration phase of a malignant tumor when it spreads throughout the body through circulatory channels. In the angiogenesis phase, the cell develops and extends during the blood supply to sustain it [5]. One in four of all malignancies in women worldwide currently occurs as a result of breast cancer. The incidence of breast cancer has increased by more than 20% globally since 2008, whereas the mortality rate has increased by 14% [6].

DTX, a taxane compound, has been successfully used in the treatment of metastatic, adjuvant, and neoadjuvant breast cancer in clinical trials. It is a semi-synthetic drug first discovered as a substitute for paclitaxel in 1986 [7]. DTX is an anticancer drug often used to treat prostate, ovarian, breast, and advanced non-small cell lung cancer [8]. It operates by destroying the cellular microtubular network required for mitotic and interphase cellular processes [9]. Its use is restricted due to its non-specific distribution, poor water solubility, low bioavailability, and significant adverse effects [10, 11]. To overcome these issues, nanocarriers have been actively studied in recent years because of their significant potential in the field of novel drug delivery [12].

Nanotechnology is one of the most promising technologies of the twenty-first century [13]. Liposomes, niosomes, solid lipid nanoparticles (SLN), dendrimers, polymeric nanoparticles, polymeric micelles, carbon nanotubes, nanocrystals, and other nano-carrier drug delivery systems have shown encouraging outcomes in the development of anticancer treatments [14]. One of the most efficient carriers among them is niosomes. The unique bilayer structure, self-association of non-ionic surfactants, and cholesterol in an aqueous phase make them the most potential drug carriers [12].

Niosomes' biocompatible, non-immunogenic, and biodegradable nature and flexibility in their structural characterization make them ideal for the exploration of anticancer drug delivery. They last a long time, are incredibly stable, and allow for targeted, controlled as well as sustained delivery of drugs [15, 16]. Compared with liposomes, niosomes have advantages such as good stability, low cost, easy to be formulated, and scaling-up. Lü et al. [14] successfully fabricated DTX niosomes by ethanol injection followed by lyophilization using Span® 40, Span®60, and Solutol® HS15 with a narrow range of size distribution and a high percentage of drug entrapment efficiency (%EE). The major limitation of the ethanol injection technique reported was the presence of a

small amount of ethanol in the vesicle suspension which was difficult to remove. In addition, ethanol causes liver cirrhosis, disturbs the nervous system; affects the glands in humans, and mutations (genetic changes). Several reported studies indicated the inhibitory effects of DTX on the breast cancer Michigan Cancer Foundation-7 (MCF-7) cell lines.

Several studies have reported that pluronic surfactants themselves prolong the residence time and decrease the clearance rate of the drug, resulting in drastic sensitization of these tumors concerning various anticancer drugs [17]. Hence, the current research work was aimed to fabricate and characterize the DTX-loaded niosomes using Sorbitan Monopalmitate (Span® 40) and Pluronic® F108 (PF108) and evaluate their efficiency on the breast cancer cells. A 3^2 full factorial design was employed to fabricate the DTX-loaded niosomes. The developed DTX niosomes were investigated for solubility issues, and anticancer effects on breast cancer were further tested for particle size, polydispersity index (PDI), %EE, hemolysis, and stability studies.

Methods

Materials

IQ-GenX, Navi Mumbai, India, generously provided DTX. Cholesterol, PF108, and Span®40 were generous gift samples from Molychem Lab, Mumbai. Methanol, chloroform, and distilled water were supplied by Fine Chemical, Mumbai.

Preparation of niosomes

A thin-layer evaporation technique was used to fabricate DTX niosomes. DTX, Span® 40, and PF108 were dissolved in a solution of 8 mL methanol and 2 mL chloroform. This admixture was magnetically stirred for 30 min and the resultant solution was allowed to evaporate for over 1 h in a rotary evaporator that resulted in a thin film. The flask was held in a vacuum for 30 min to obtain a fully dried film. The film was hydrated with 20 mL of distilled water and the solution was extensively vortexed and mixed for 20 min. The resulting solution was centrifuged for 5 min at 8000 rpm, the supernatant was separated and the DTX niosomes were freeze-dried and stored in a refrigerator at 2–8 °C.

3^2 factorial design

The effect of the formulation variables, each at three levels, and nine different combinations were investigated using a 3^2 full factorial design. The concentration of Span® 40 (X_1) and cholesterol (X_2) was employed as independent variables, whereas particle size (Y_1) and %*EE* (Y_2) were the dependent variables [18].

Characterization of DTX niosomes

Particle size and polydispersity index

The particle size and PDI of all freshly prepared DTX-loaded niosomal formulations were determined by using Zetasizer version 11 (Malvern Instruments, Worcestershire, UK) with the manufacturer's software [19].

Percent entrapment efficiency

DTX niosome's %EE was determined using the centrifugation process. At room temperature, the freshly fabricated formulations were centrifuged for 10 min at 20,000 rpm. The supernatant was diluted sufficiently by adding methanol and the absorbance was recorded at 230 nm employing a UV–visible spectrophotometer (Shimadzu UV-1900) [20].

Zeta potential

The zeta potential of DTX-loaded niosomes was measured using the Zetasizer (Horiba SZ-100). The samples were diluted at a 1:1 ratio using distilled water. The samples were transferred to cuvettes and were then placed in the Dynamic Light Scattering (DLS) analyzer to measure zeta potential [21].

Transmission electron microscopy

Transmission electron microscopy (TEM) (Jeol Model JM 2100) was used to examine the morphological characteristics of the optimized DTX niosomes. A drop of niosomal formulation was placed on a carbon-coated copper sheet, and the unwanted sample was wiped away using filter paper. The carbon grid was stained with a drop of staining factor (2%w/v solution for phosphotungstic acid) and left aside for 2 min. The excess staining agent was transferred to filter paper, and an electron microscope was employed to observe the thin film of stained niosomes [22].

Fourier transform infrared spectroscopy

Fourier Transform Infrared (FTIR) spectroscopy was used to determine the compatibility of DTX with excipients. Briefly, about 2 mg of a sample was ground thoroughly with previously dried potassium bromide (KBr) at 120 °C for 30 min, uniformly mixed and compressed into disks, and kept in the sample holder. Later, the disks were scanned at the wavelength of 4000–500 cm^{-1}. Plain DTX and DTX niosomes were assessed using an FTIR spectrophotometer (Agilent, Alpha 100508) to obtain FTIR spectrums [23].

Differential scanning calorimetry

The thermal behavior of plain DTX and optimized DTX niosomes were examined using an automatic

differential scanning calorimeter (DSC) (Pyris Diamond TG/DTA, Perkin Elmer) equipped with an intracooler. A platinum crucible was used with an alpha-alumina powder as a reference to calibrate the DSC temperature and enthalpy scale. The powder samples of 3–5 mg were weighed and hermetically kept in the pierced aluminum pan and heated at a constant rate of 10 °C/min over a temperature range of 10 °C to 500 °C. Nitrogen was used at the flow rate of 150 mL/min to create an inert atmosphere. The reference employed for determination was an empty aluminum pan (SDT Q600 V20.9 Build 20) [24].

X-ray diffraction

Plain DTX and DTX niosomes were compared in the crystallographic investigation using an X-ray diffractometry (XRD) (Bruker D8 Advance) with Cu-K radiation ($\lambda = 1.54$) at a voltage of 40 kV, 50 mA, at increments of 0.02° from 5° to 100° diffraction angle (2θ) at 1 s/step. Plain DTX and optimized DTX niosomes were scanned against a zero backdrop [25].

In vitro drug release study

The pattern of release of plain DTX and DTX niosomal formulation was determined using the dialysis method [26–28]. The DTX solution equal to 2.5 mg DTX was poured into (12,000 Da MWCO) dialysis tubes and tightly sealed. The solution-filled dialysis tubes were placed in 100 mL phosphate buffer saline (PBS) (pH 7.4). Accurately 5 mL samples were withdrawn for estimation at 1, 2, 4, 8, 12, and 24 h. The volume of the drug release medium was maintained at 100 mL by substituting it with equal volumes of the fresh medium while stirring with a magnetic stirrer at 200 rpm/min. The withdrawn samples were centrifuged at 2000 rpm for 5 min, and the supernatant was separated and analyzed using a UV–visible spectrophotometer at 230 nm to estimate the percentage of drug released.

In vitro cytotoxicity study

The cytotoxicity of plain DTX and DTX niosomal formulation was investigated against the MCF-7 cell line. A 3-(4, 5-dimethylthiazol-2-yl)-2, 5-diphenyl tetrazolium bromide (MTT) dye reduction test was used to evaluate in vitro cytotoxicity. The cells were attacked and started growing again after being cultured for 24 h at 37 °C in a 5% CO_2 incubator. Accurately 100 µl of serially diluted test solutions and plain DTX solution were substituted for supernatant Dulbecco's Modified Eagle Medium (DMEM) in the niosomal formulation. Under the same conditions, all of the well plates were incubated for 48 h. After incubation, the supernatants were replaced with the same volume of MTT stock solution made in 0.6 mg/mL PBS. After 4 h of incubation, the MTT solution was changed for the same volume of dimethyl sulfoxide (DMSO). The resulting absorbance of DMSO solutions was reported at 590 nm using an enzyme-linked immunosorbent assay (ELISA) plate reader. Further, IC_{50} values were calculated using dose–response curves, and the absorbance of test samples and untreated cells was measured and compared [29–31].

Stability study

Short-term stability analysis of plain DTX and an optimized DTX niosome formulation was performed as per ICH Q1A R2 stability study guidelines. The stability of the DTX niosomes was investigated by storing them at 5 ± 3 °C and 25 ± 2 °C/ 75% relative humidity (RH) for a total of 3 months [22].

Results

DTX niosomes were prepared by using DTX, Span® 40, PF108, and the mixture of methanol and chloroform by using the thin-layer evaporation method. The technique of thin film hydration was used to prepare niosomes as it produces multilamellar non-ionic niosomal vesicles. Besides, it is the most efficient, simple, and reproducible method. To fabricate niosomes with a narrow size distribution, it is typically combined with sonication [34]. Historically, a variety of non-ionic surfactants have been employed to decrease the particle size and enhance the zeta potential of drug-free niosomal formulations [31]. Cholesterol, as it interacts with non-ionic surfactants, was used in the right proportion to produce the most stable formulation with an improved niosomal mechanical strength as well as water permeability that will retain its integrity under high-stress conditions [35]. Span® 40 is a hydrophobic amphiphile with a HLB value of 6.7, and DTX is also hydrophobic. Therefore, when pluronic F108 which has a lower molecular weight and owns a longer hydrophilic PEO chain than the PPO chain, increases the hydrophobicity level, thus contributing to drug loading [34]. Niosomes, as they assist to direct the drug to the cancer cells, lengthen the course of treatment with lowered severity of harmful side effects, and enhance drug stability, are a promising drug delivery carrier for cancer therapy [32].

Formulation design

The combined effect of two formulation variables, each at three levels, and the potential nine DTX niosome formulation combinations were investigated using a 3^2 factorial design. Cholesterol (X_1) and Span® 40 (X_2) concentrations were the independent variables while the particle size (Y_1) and percent EE (Y_2) were the dependent

variables in this experiment. The optimized batch (F5) showed 97.43% percent EE and a particle size of 244.9 nm.

Effect of formulation variables

The results of the investigations indicate that the response values of the dependent variables vary with the change in independent variables. This is also affected by the spacious area of coefficient values of the polynomial equation terms for Y_1. The major outcomes of X_1 and X_2 describe the typical outcome of increasing one variable from a low to a high level. Out of the 9 formulations, the particle size (Y_1) and %*EE* (Y_2) values displayed a large range from 531.6 to 244.9 nm and 66.55 to 97.43%, respectively. It clearly shows that the Y_1 and Y_2 values were highly influenced by the X_1 and X_2 variables chosen for the trials. This could also be illustrated by a wide variety of responses for the coefficients of the terms in equations. The primary effects of X_1 and X_2 indicate the average result of adjusting one variable at a time from low to high. The complete model statistical analysis shown in Table 1 reveals the significant influence of independent variables on the dependent variables.

Analysis of variance (ANOVA)

The statistical validity of the polynomials was determined using the Design Expert® software's ANOVA feature. Mathematical designs were created for each response and verified for significance. The adjusted R^2 and predicted R^2 values were in best recommendations for all responses, showing that the mathematical model accurately predicted the outcomes. The degree of variation in the dependent variable is determined by the independent variables, and it is collectively depicted by polynomial equations. The statistical model generated interactive polynomial terms for each response; the equations are as follows:

$$Y = \beta_0 + \beta_1 A + \beta_2 B + \beta_3 AB + \beta_4 A^2 + \beta_5 B^2 \quad (1)$$

where Y is the independent variable, β_0 represents the arithmetic mean response of the 9 trials, and β_1 is the calculated factor of a coefficient. The average outcome when the components were adjusted one at a time from their lower to higher values is represented by the principal effects of the degree of A and B. The interaction terms (AB) demonstrated how the outcomes vary when two variables are altered at the same time. The DoE data suggest that particle size and %*EE* depend on the selected independent variables. The following polynomial equations were used to derive conclusions based on the statistical sign it bears demonstrating synergistic or antagonistic effects (Table 2).

$$Y_1(\text{particle size}) = 244.90 + 24.79A + 1.65B + 70.44AB + 107.86A^2 + 91.48B^2 \quad (2)$$

$$Y_2(\%EE) = 97.43 + 4.58A + 0.3394B + 3.51AB - 10.51A^2 - 4.75B^2 \quad (3)$$

Table 1 Experimental design of DTX niosomes and effect on dependent variables

Formulation code	Factor 1 Cholesterol (X_1) (mg)	Factor 2 Span® 40 (X_2) (mg)	Response 1 Particle size (nm)	Response 2 EE (%)
F1	2	2	444.5 ± 2.5	83.56 ± 1.2
F2	2	2.5	421.8 ± 1.3	76.95 ± 1.3
F3	2	3	489.0 ± 0.9	66.55 ± 0.4
F4	2.5	2	412.0 ± 1.1	86.31 ± 0.9
F5	2.5	2.5	244.9 ± 0.5	97.43 ± 1.2
F6	2.5	3	531.6 ± 1.2	89.69 ± 1.1
F7	3	2	518.0 ± 1.3	82.26 ± 0.8
F8	3	2.5	346.0 ± 1.7	84.37 ± 0.7
F9	3	3	391.5 ± 1.4	87.65 ± 1.2

Table 2 ANOVA for a quadratic model of particle size and %EE

Source	D_f	Particle size				%EE			
		Sum of squares	Mean square	*F*-value	*P*-value	Sum of squares	Mean square	*F*-value	*P*-value
Model	5	61,182.5	12,236.5	11.36	0.036	55,780	111.58	10.80	0.039

The model *F*-value of 11.36 and 10.80 for particle size and %*EE*, respectively, indicates its significance. Because of the noise, there is only a 3.64% chance that such high *F*-values will occur. The *P*-values for the model were < 0.05. The terms AB, A^2, and B^2 are important model variables in this scenario. The fit statistics values for the model are presented in Table 3. Adequate precision tests the ratio of a signal to noise. A ratio of more than 4 would be desirable. Thus, the ratio 11.054 shows a suitable signal. The space of the design may be navigated using this model. *A* coefficient of variation (CV) for a single variable describes the dispersion of the variable. The lower CV describes the smaller residuals relative to the predicted value suggesting a good model fit.

Counter plot and 3D surface plot analysis

The data are presented as 2D contour plots and 3D response surface plots for understanding interactions between the components and their impacts on the responses. These plots are useful in predicting the impact of two factors on the same set of results at the same time. The effects of change in concentrations of independent variables on particle size and %EE are described in the following section.

Effect on particle size

Cholesterol is an essential parameter in the fabrication of niosomal vesicles. Altering the concentration of cholesterol and Span® 40 can alter the particle size. The counterplot presented in Fig. 1A represents the design space for employing independent variables based on particle size.

Effect on percent entrapment efficiency

At the initial phase of experiments, where the concentration of Span® 40 increases the %*EE* also increases. However, additional increases in the Span® 40 concentration led to a decrease in DTX %*EE*. Amongst independent variables investigated, %*EE* was affected mainly due to cholesterol concentration, Fig. 2. The %*EE* was found to be 97.43 ± 1.2 in the F5 batch hence it was considered as an optimized batch [30].

Particle size analysis and polydispersity index

The particle size of the optimized DTX niosomal formulation (*F5*) was found to be 244.9 nm. Figure 3 PDI is a representation of the distribution of particle size within a given sample. The particle size distribution ranged from 244.9 to 531.6 nm. The numerical value of PDI was 0.75 indicating monodisperse samples.

Table 3 Fit statistics for particle size and %EE

Particle size				%EE			
SD	**32.81**	R^2	**0.9498**	**SD**	**3.21**	R^2	**0.9474**
Mean	422.09	Adjusted R^2	0.866	Mean	83.86	Adjusted R^2	0.8596
CV%	7.78	Predicted R^2	NA[(1)]	CV%	3.83	Predicted R^2	NA[(1)]
		Adeq Precision	11.053			Adeq Precision	10.477

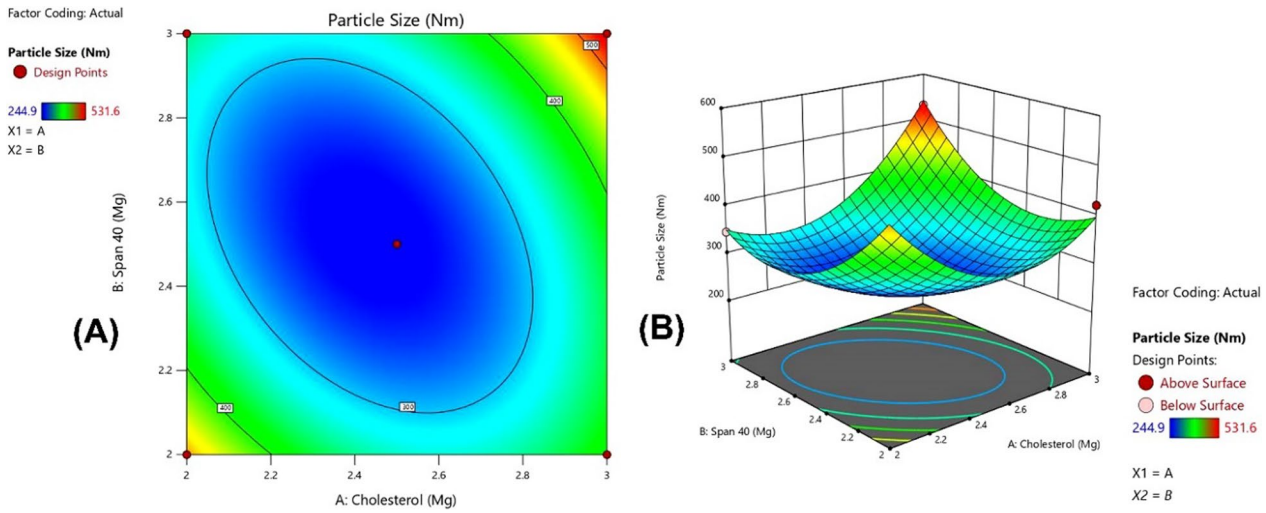

Fig. 1 **A** Counter plot and; **B** 3D surface response plot for particle size

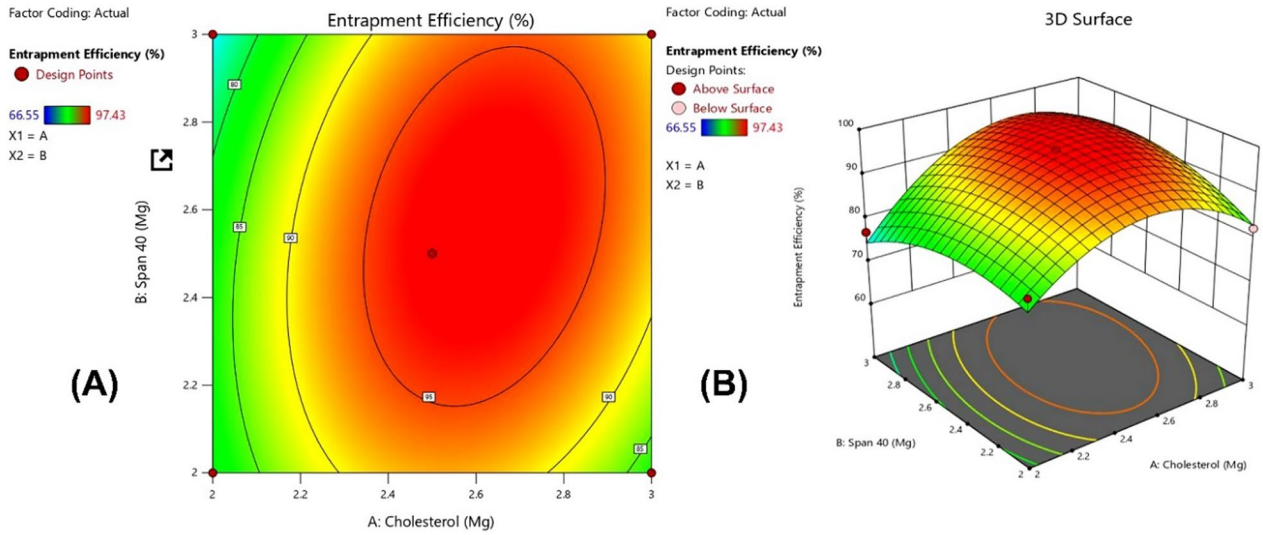

Fig. 2 **A** Counter plot and, **B** 3D surface response plot %EE of DTX niosomes

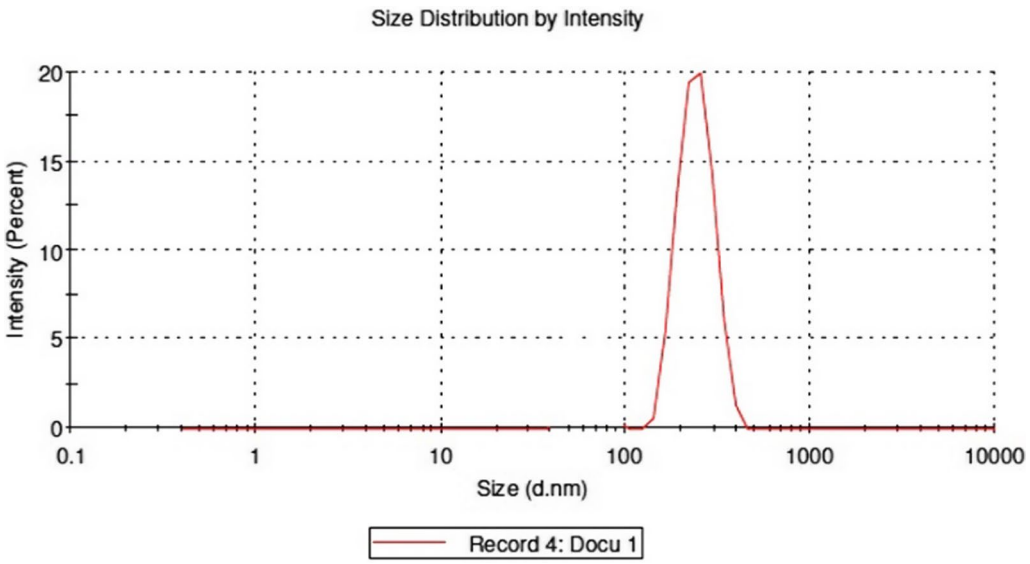

Fig. 3 The particle size of DTX co-loaded niosomes

Zeta potential

The zeta potential distribution graph of DTX-loaded niosomes is presented in Fig. 4. Niosomes were negatively charged with a zeta potential of about − 10 mV [37].

Transmission electron microscopy

The TEM images of optimized DTX-loaded niosomes formulations (F5) are exhibited in Fig. 5. Niosomes appeared as well-defined spheres with a distinct wall enclosing an aqueous core [38]. Furthermore, the mean niosome size determined by TEM agreed well with that determined by particle size and PDI experiments.

Fourier transform infrared spectroscopy

The FTIR spectra of DTX and DTX-loaded niosomal formulation were recorded in the range of 4000–400 cm^{-1}. In DTX FTIR spectra, the peaks at 3010 cm^{-1} and 1502 cm^{-1} are the characteristic peaks of the benzene ring and 1699 cm^{-1} indicates the presence of (C=O) carbonyl group in the DTX. The FTIR spectrum of optimized niosomal formulation (F5) is presented in Fig. 6.

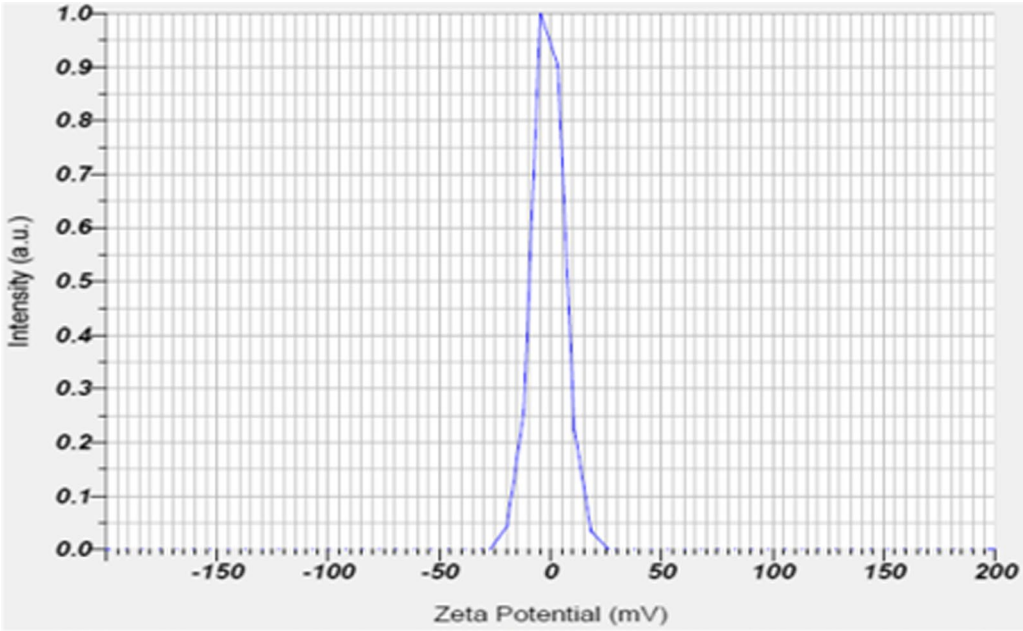

Fig. 4 Zeta potential of optimized DTX niosomal formulation (F5)

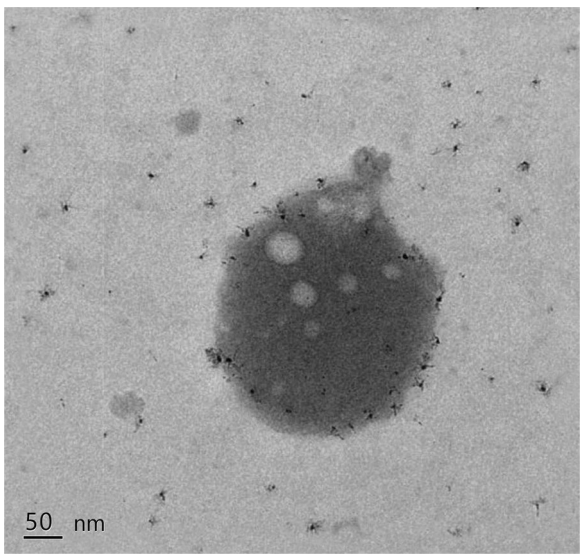

Fig. 5 TEM image of optimized DTX niosomal formulation (F5)

Differential scanning calorimetry

The melting point temperature of DTX and DTX niosomal formulation were recorded using DSC (SDT Q600 V20.9 Build 20). The DTX DSC thermogram showed a high endothermic peak at 178-188 °C that corresponds to the DTX melting. DSC thermograms of DTX-loaded niosomal dispersion interestingly displayed endotherm at 90.46 and 103 °C corresponding to Span® 40, and cholesterol (Fig. 7).

X-ray diffractometry

Figure 8A and B showed the P-XRD pattern of plain DTX and optimized niosomal formulation batch (F5), respectively. The results obtained from the P-XRD study were in agreement with DSC studies. DTX is a white crystalline powder with multiple distinct peaks at varied relative intensities when viewed via a diffraction angle which disappeared in the P-XRD of the DTX niosomal formulation (F5) [30].

In vitro drug release study

The in vitro drug release from plain DTX and DTX niosomes is presented in Fig. 9. The highest percentage of cumulative drug released in solution from the plain DTX was 85% after 8 h and from DTX co-loaded niosome was 35.2% after 24 h [39].

In vitro cytotoxicity study

The in vitro cytotoxicity of plain DTX and optimized DTX niosomal formulation (F5) was evaluated in the MCF-7 cells using the MTT assay. The findings of the study are reported as half-maximal inhibitory concentration (IC_{50}). The doses of DTX ranged from 0.0001 to 1 µM. In vitro cytotoxicity of DTX was strongly influenced by drug concentration. In the cell line study, both plain DTX and DTX niosomes successfully inhibited the proliferation in a concentration-dependent manner. IC_{50} of MCF-7 cells were more responsive to DTX niosomes, as compared to IC_{50} of plain DTX indicating sustained

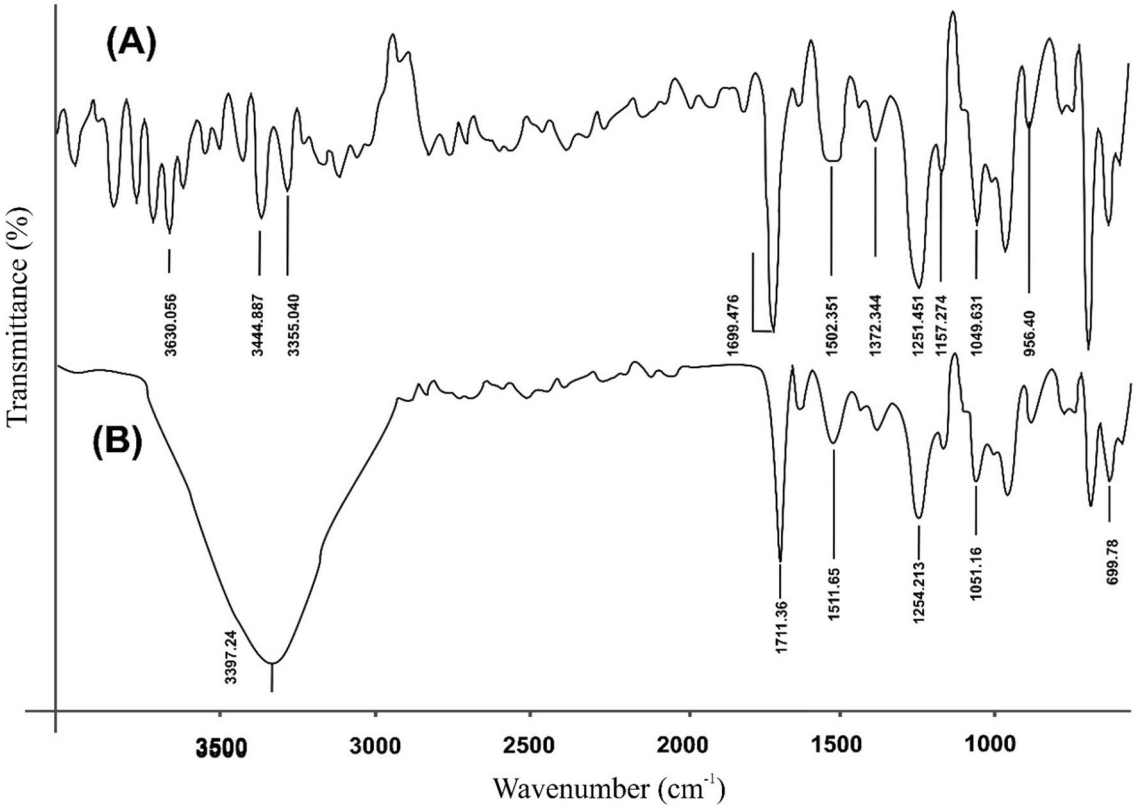

Fig. 6 FTIR overlay spectra of (**A**) plain DTX (**B**) optimized DTX niosomal formulation (F5)

release of DTX from niosomes over a prolonged time (Fig. 10).

Stability study

The stability of niosomal formulations was investigated by keeping track of changes in the physical appearances and %*EE* by storing them at a temperature of 2–8 °C for 3 months. At the end of the study, there was no significant change in the appearance, particle size, PDI, and zeta potential of the niosomal formulations indicating their better stability. Additionally, DTX content retained throughout 1, 2, and 3 months was 97.20 ± 0.9, 97.13 ± 1.1, and 97.02 ± 0.7%, respectively, against the initial amount of 97.43 ± 1.2%. The plain DTX retained only 80% 0.25 ± 0.3% of its initial 98.52 ± 0.9% indicating niosomes superior stability over plain DTX.

Discussion

DTX is indicated for the treatment of individuals with locally advanced or metastatic breast or non-small-cell lung cancer, as well as androgen-independent advanced or metastatic cancer. Its application in the treatment of cancer is constrained by its poor solubility, significant adverse effects, and multidrug resistance (MDR) [30]. Although many researchers have successfully developed DTX liposomes, one of the main problems with those traditional liposomes was rapid blood clearance of DTX because of the adsorption on plasma proteins, drug leakage, and high production costs [40]. Compared with liposomes, niosomes have been reported to possess good stability, low cost, and ease of formulation and scale-up. Niosomes are much more stable because their forming materials are non-ionic surfactants that are more stable than those of lipids used in liposomes, both in terms of physical and chemical stability [22]. Therefore, to address these problems and improve therapeutic efficacy, DTX was encapsulated in niosomes.

The thin-layer technique has the advantage of being much faster processing and requiring smaller quantities of lipids for analysis. The rotary evaporator takes advantage of the low boiling points of solvents by creating an environment where the solvent rapidly boils off leaving only the product. A big advantage of rotary evaporation is the easy possibility of scaling up [41].

The 3^2 factorial design applied at three levels led to potential nine DTX niosomal combinations. In these trials, the concentrations of cholesterol (X_1) and Span® 40 (X_2) served as independent variables, and the dependent

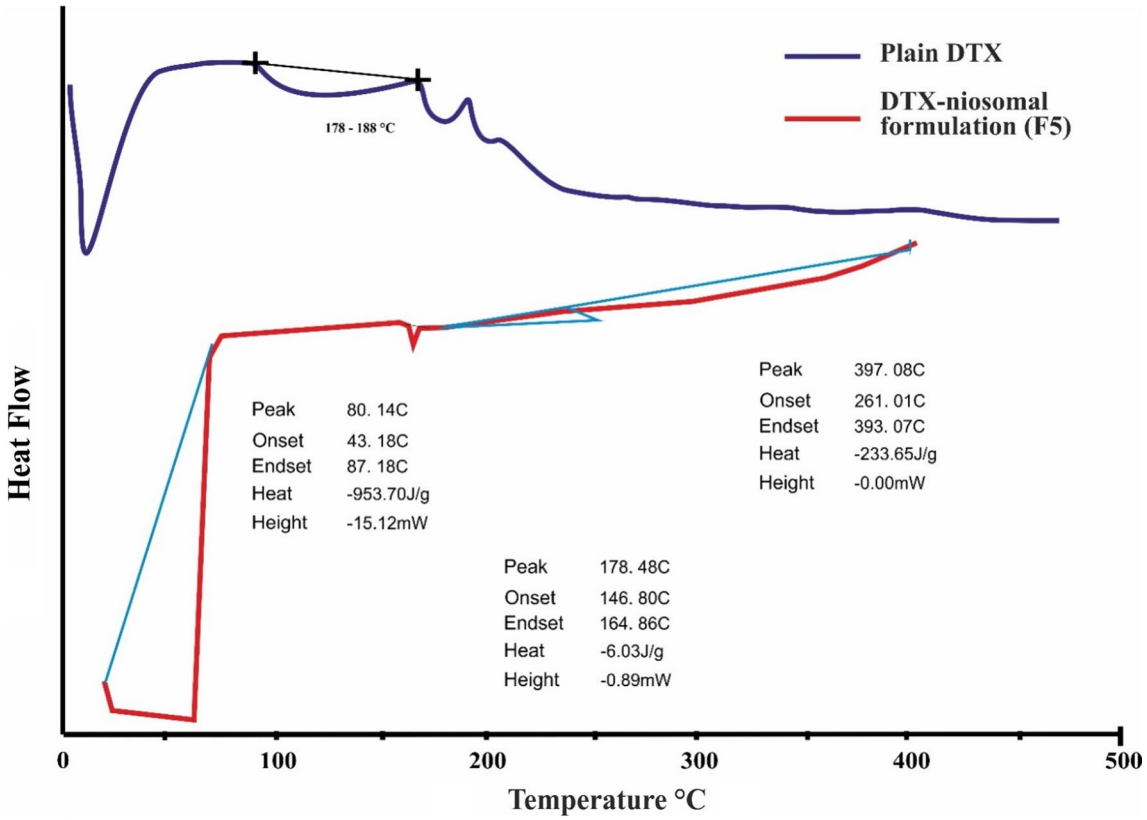

Fig. 7 DSC of (**A**) plain DTX; and (**B**) DTX niosomal formulation (F5)

variables were particle size (Y_1) and %*EE* (Y_2). The particle size of niosomes ranged from 244.9 to 531.6 nm. Further, the drug's cytotoxicity against cancer cells is enhanced by decreasing the particle size and increasing the amount of drug enclosed in the niosome's vesicles [36]. There is an inverse relationship between concentrations of Span® 40 and cholesterol in combination and particle size. The %*EE* was found to be highest in the F5 batch which indicates an increase in the cholesterol concentration further increased %*EE*. It might be attributed to the high concentration of cholesterol preventing the gel state from transforming into a liquid-ordered state, which increases the stiffness of the resultant bilayers and hence increases niosomes stability and %*EE* [30]. The cholesterol and Span® 40 concentration ratio in the optimized formulation was found to be 2.5:2.5. These results were in significant agreement with the particle size, zeta potential, and PDI of DTX niosomes prepared by using Span® 40 as a polymeric surfactant [37]. The negative value of zeta potential indicated that the appropriate concentration of Span® 40 and cholesterol was significantly effective for loading vesicles. The zeta potential of niosomes decreased as the amount of Span® 40 and cholesterol increased, probably because the molecular weight for PF108 distribution onto the bilayer surfactant structure increased [38].

The TEM images revealed a well-defined spherical form with a distinct wall enclosing an aqueous center, which was consistent with the findings reported earlier for rifampicin-loaded niosomes [22]. In the DSC thermograms, the lack of a DTX melting endotherm in the formulation indicated that the drug has changed from crystalline to amorphous which could be correlated to improved DTX entrapment in niosomal formulation [41, 42]. The P-XRD pattern of DTX was robust and distinctive, indicating that it was a crystalline powder. On the other hand, the optimized DTX niosomal formulation (F5) revealed a reduction in peaks and increased diffusive peaks, indicating an amorphous form of DTX [30, 36, 43]. Niosomes have many advantages common to all vesicular systems such as prolongation of the circulation of entrapped drugs, possible targeting to special organs and tissues and controlled release of entrapped drugs, and being biodegradable and non-immunogenic [39]. In the in vitro drug release study, the amount of DTX released from niosomes concerning time was reduced, and at the same time, the release was sustained. The low DTX release in the blood circulation would help to target

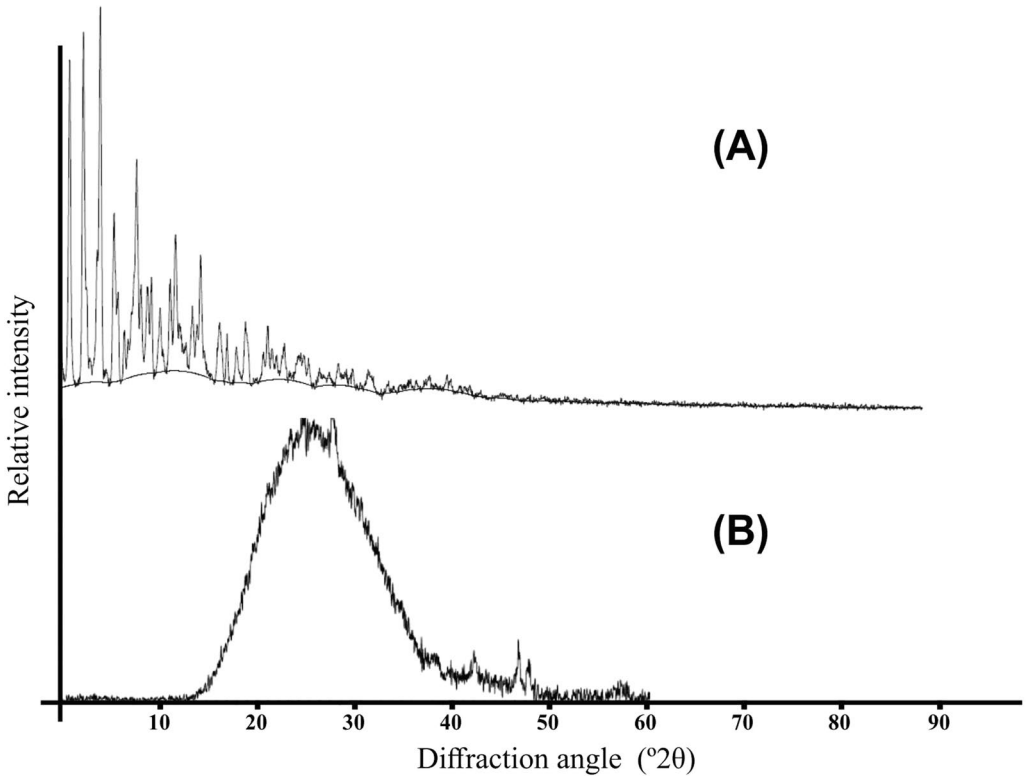

Fig. 8 P-XRD of (**A**) plain DTX; and (**B**) DTX optimized niosomal formulation (F5)

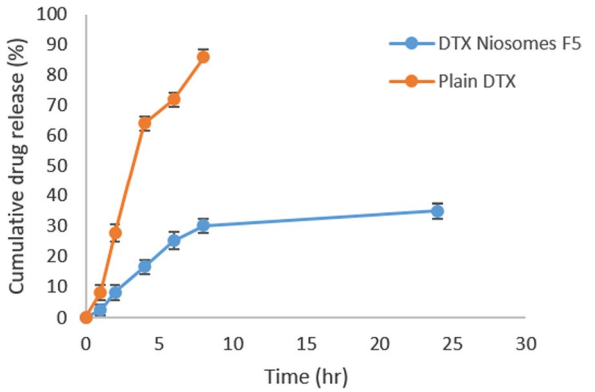

Fig. 9 Graphical presentation of cumulative drug release study

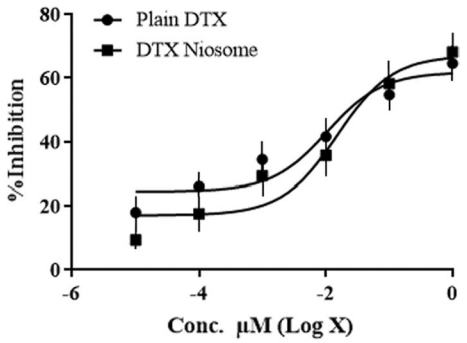

Fig. 10 Cytotoxicity study plain DTX and optimized DTX niosomal formulation (F5)

increased drug concentration to cancer cells and therefore would meet the parameters for effective drug delivery in cancer treatment [39].

A cytotoxicity study reveals that the DTX niosomes significantly induce cytotoxicity in MCF-7 cells indicating the effectiveness of F5 formulation. It showed a sustained DTX delivery for 24 h which help to avoid its premature release to reduce the toxicity [31, 36]. The formulation's stability studied at 2–8 °C showed its physical integrity retaining a good amount of drug that was speculated as stable over the storage period.

Conclusion

Niosomal formulations under study proved to have the potential to improve the aqueous solubility of the DTX due to the pre-dissolved form of the drug in the polymer and its monodisperse nanometric size. DTX niosomes were successfully released DTX in a sustained manner which avoids high-concentration toxicity to the

normal cells and delivers the drug slowly at the site of action. Besides, the stability of the DTX was improved when it was formulated in the niosomal form. Thus, DTX niosomes are a promising approach for the solubility enhancement, toxicity reduction, and stability enhancement of the anticancer drug DTX.

Abbreviations

DTX	Docetaxel
%EE	Percent entrapment efficiency
SLN	Solid lipid nanoparticles
MCF-7	Michigan Cancer Foundation-7
WHO	World Health Organization
PF108	Pluronic® F108
Span 40	Sorbitan monopalmitate
PDI	Polydispersity index
RPM	Revolutions per minute
DLS	Dynamic light scattering
TEM	Transmission electron microscope
FTIR	Fourier transform infrared
KBr	Potassium bromide
DSC	Differential scanning calorimeter
P-XRD	Powder X-ray diffractometer
PBS	Phosphate buffer saline
MTT	3-(4,5-Dimethylthiazol-2-yl)-2, 5-diphenyl tetrazolium bromide
DMEM	Dulbecco's Modified Eagle Medium
DMSO	Dimethyl sulfoxide
ELISA	Enzyme-linked immunosorbent assay
RH	Relative humidity
MDR	Multi-drug resistance

Acknowledgements
The authors thank Tatyasaheb Kore College of Pharmacy, Warananagar, India, and its other stakeholders for providing timely help, guidance, and research amenities.

Author contributions
RDC, DSG, and KSP conceptualized the study and literature survey, manuscript writing, statistical analysis, data interpretation along with proofreading. AAH and JID performed data interpretation and proofreading. RDC and KSP prepared the manuscript, performed statistical analysis, interpreted the data, and proofread the manuscript. All authors have read and approved the final manuscript.

Funding
Not applicable.

Availability of data and materials
The datasets used and/or analyzed during the current study are available from the corresponding author upon reasonable request.

Declarations

Ethics approval and consent to participate
Not applicable.

Competing interests
The authors declare that they have no competing interests.

Author details
[1]Department of Pharmaceutical Quality Assurance, Tatyasaheb Kore College of Pharmacy, Panhala, Kolhapur, Warananagar, Maharashtra 416113, India. [2]Department of Pharmaceutical Technology, Bharati Vidyapeeth College of Pharmacy, Near Chitranagari, Kolhapur, Maharashtra 416013, India. [3]Department of Pharmaceutics, Tatyasaheb Kore College of Pharmacy, Warananagar, Maharashtra 416113, India.

Received: 21 December 2022 Accepted: 16 May 2023
Published online: 24 May 2023

References

1. Xiaomei M, Herbert Y (2006) Global burden of cancer. Yale J Biol Med 79(3–4):85–94
2. Siegel R, Miller K, Fuchs H, Jemal A (2021) Cancer Statistics, 2021. CA A Cancer J Clin 71(1):7–33. https://doi.org/10.3322/caac.21654
3. Aguilera F (2017) Neoplasia in mollusks: what does it tell us about cancer in humans? A review. J Genet Disord 1(7):558
4. Kasper D, Fauci A, Hauser S, Longo D, Jameson J, Loscalzo J (2015) Harrison's principles of internal medicine. Mcgraw-hill, New York
5. Nobili S, Lippi D, Witort E, Donnini M, Bausi L, Mini E, Capaccioli S (2009) Natural compounds for cancer treatment and prevention. Pharmacol Res 59:365–378
6. Wong HL, Bendayan R, Rauth AM, Li Y, Wu XY (2007) Chemotherapy with anticancer drugs encapsulated in solid lipid nanoparticles. Adv Drug Deliv Rev 59(6):491–504
7. Bissery MC, Nohynek G, Sanderink GJ, Lavelle F (1995) Docetaxel (Taxotere): a review of preclinical and clinical experience. Part I: preclinical experience. Anticancer Drugs 6:339–355
8. He X, Li C, Wu X, Yang G (2015) Docetaxel inhibits the proliferation of non-small-cell lung cancer cells via upregulation of microRNA-7 expression. Int J Clin Exp Pathol 8:9072–9080
9. Bates D, Eastman A (2017) Microtubule destabilising agents: far more than just antimitotic anticancer drugs. Br J Clin Pharmacol 83(2):255–268
10. Sohail MF, Rehman M, Sarwar HS et al (2018) Advancements in the oral delivery of Docetaxel: challenges, current state-of-the-art, and future trends. Int J Nanomed 13:3145–3161
11. Wei QY, Xu YM, Lau ATY (2020) Recent progress of nanocarrier-based therapy for solid malignancies. Cancers (Basel) 12:1–37
12. Mishra B, Patel BB, Tiwari S (2010) Colloidal nanocarriers: a review on formulation technology, types and applications toward targeted drug delivery. Nanomedicine 6(1):9–24
13. Yeo P, Lim C, Chye S, Kiong Ling A, Koh R (2017) Niosomes: a review of their structure, properties, methods of preparation, and medical applications. Asian Biomed 11(4):301–314
14. Din FU, Aman W, Ullah I et al (2017) Effective use of nanocarriers as drug delivery systems for the treatment of selected tumors. Int J Nanomed 12:7291–7309
15. Mahale NB, Thakkar PD, Mali RG, Walunj DR, Chaudhari SR (2012) Niosomes: novel sustained release nonionic stable vesicular systems—an overview. Adv Colloid Interface Sci 183:46–54
16. Su J, Chen F, Cryns VL, Messersmith PB (2011) Catechol polymers for pH-responsive, targeted drug delivery to cancer cells. J Am Chem Soc 133:11850–11853
17. Batrakova EV, Kabanov AV (2008) Pluronic block copolymers: evolution of drug delivery concept from inert nanocarriers to biological response modifiers. J Control Release 130(2):98–106. https://doi.org/10.1016/j.jconrel.2008.04.013
18. Haider MD, Kanoujia J (2015) Pioglitazone loaded vesicular carriers for anti-diabetic activity: development and optimization as per central composite design. Int J Pharm Pharm Sci 5:2333–3715
19. Mehta SK, Jindal N (2020) Formulation of Tyloxapol niosomes for encapsulation, stabilization and dissolution of anti-tubercular drugs. Colloids Surf B Biointerfaces 101:434–441
20. Khan MI, Madni A (2015) ATR- FTIR based per and post formulation compatibility studies for the design of niosomal drug delivery system containing nonionic amphiphile and chrondroprotectiove drug. J Chem Soc 5:527–535
21. Shilakari G, Asthana A, Sharma P (2012) *In Vitro* and *In Vivo* evaluation of niosomal formulation for controlled delivery of clarithromycin. Hindawi Publishing Corporation Scientifica, New York, pp 1–10
22. Khan DH, Bashir S, Figueiredo P, Santos HA, Khan MI, Peltonen L (2019) Process optimization of ecological probe sonication technique for production of rifampicin loaded niosomes. J Drug Deliv Sci Technol 50:27–33
23. Bayindir ZS, Yuksel N (2010) Characterization of niosomes prepared with various nonionic surfactants for paclitaxel oral delivery. J Pharm Sci 99(4):2049–2060

24. Khan MI, Madni A, Peltonen L (2016) Development and *in vitro* characterization of sorbitan monolaurate and poloxamer 184 based niosomes for oral delivery of diacerein. Eur J Pharm Sci 95:88–95
25. Sayeda SSA, Asha AN, Kusum DV (2019) Formulation and evaluation of niosomes of mirtazapine for nasal delivery. Indo Am J Pharm 5:2031–2011
26. Barani M, Mirzaei M, Torkzadeh-Mahani M, Adeli-Sardou M (2019) Evaluation of Carum-loaded niosomes on breast cancer cells: Physicochemical properties, *in vitro* cytotoxicity, flow cytometric, DNA fragmentation and cell migration assay. Sci Rep [Internet] 9(1):7139
27. Nazari-Vanani R, Karimian K (2019) Capecitabine-loaded nanoniosomes and evaluation of anticancer efficacy, artificial Cells. Nanomed Biotechnol 47(1):420–426
28. Sezgin-Bayindir Z, Onay-Besikci A, Vural N, Yuksel N (2013) Niosomes encapsulating paclitaxel for oral bioavailability enhancement: preparation, characterization, pharmacokinetics and biodistribution. J Microencapsul 30(8):796–804
29. ManjappaAS KPS (2019) Ameliorated *in vitro* anticancer efficacy of methotrexate D-α-Tocopheryl polyethylene glycol 1000 succinate ester against breast cancer cells. Future J Pharm Sci 5:1–10
30. Patil KS, Hajare AA, Manjappa AS, More HN, Disouza JI (2021) Design, development, *in silico* and *in vitro* characterization of Docetaxel-loaded TPGS/Pluronic F 108 mixed micelles for improved cancer treatment. J Drug Deliv Sci Technol 65:102685. https://doi.org/10.1016/j.jddst.2021.102685
31. Patil SS, Chougale RD, Manjappa AS, Disouza JI, Hajare AA, Patil KS (2022) Statistically developed docetaxel-laden mixed micelles for improved therapy of breast cancer. OpenNano 5:100079. https://doi.org/10.1016/j.onano.2022.100079
32. Haley B, Frenkel E (2008). Nanoparticles for drug delivery in cancer treatment. In: Urologic oncology: seminars and original investigations, vol 26, pp 57–64. https://doi.org/10.1016/j.urolonc.2007.03.015
33. Tavano L, Vivacqua M, Carito V, Muzzalupo R, Caroleo MC, Nicoletta F (2013) Doxorubicin loaded magneto-niosomes for targeted drug delivery. Colloids Surf B 102:803–807. https://doi.org/10.1016/j.colsurfb.2012.09.019
34. Ge X, Wei M, He S, Yuan WE (2019) Advances of non-ionic surfactant vesicles (niosomes) and their application in drug delivery. Pharmaceutics 11(2):55. https://doi.org/10.3390/pharmaceutics11020055
35. Ritwiset A, Krongsuk S, Johns JR (2016) Molecular structure and dynamical properties of niosome bilayers with and without cholesterol incorporation: a molecular dynamics simulation study. Appl Surf Sci 380:23–31. https://doi.org/10.1016/j.apsusc.2016.02.092
36. Patil KS, Hajare AA, Manjappa AS, More HN, Disouza JI (2022) Design, development, *in silico*, and *in vitro* characterization of camptothecin-loaded mixed micelles. *in vitro* testing of verapamil and ranolazine for repurposing as coadjuvant therapy in cancer. J Pharm Innov. https://doi.org/10.1007/s12247-022-09688-0
37. Kumar GP, Rajeshwarrao P (2011) Nonionic surfactant vesicular systems for effective drug delivery—an overview. Acta Pharm Sinica B 1(4):208–219. https://doi.org/10.1016/j.apsb.2011.09.002
38. Abdelbary G, El-Gendy N (2008) Niosome-encapsulated gentamicin for ophthalmic controlled delivery. AAPS PharmSciTech 3:740–747. https://doi.org/10.1208/s12249-008-9105-1
39. Kazi KM, Mandal AS, Biswas N, Guha A, Chatterjee S, Behera M, Kuotsu K (2010) Niosome: a future of targeted drug delivery systems. J Adv Pharm Technol Res 1(4):374. https://doi.org/10.4103/0110-5558.76435
40. Li J, Tan T, Zhao L, Liu M, You Y, Zeng Y, Chen D, Xie T, Zhang L, Fu C, Zeng Z (2020) Recent advancements in liposome-targeting strategies for the treatment of gliomas: a systematic review. ACS Appl Bio Mater 3(9):5500–5528
41. El-Ridy MS, Yehia SA, Mohsen AM, El-Awdan SA, Darwish AB (2018) Formulation of niosomal gel for enhanced transdermal lornoxicam delivery: *in vitro* and *in vivo* evaluation. Curr Drug Deliv 15(1):122–133. https://doi.org/10.2174/1567201814666170224141548
42. Hajare AA, Velapure PD, Rathod PN, Patil KS, Chopade SS (2020) Formulation and evaluation of solid lipid nanoparticle gel for topical delivery of clobetasol propionate to enhance its permeation using silk sericin as permeation enhancer. Int J Pharm Sci 11(5):2356–2365
43. Dol HS, Hajare AA, Patil KS (2022) Statistically designed novel ranolazine-loaded ethosomal transdermal gel for the treatment of angina pectoris. J Drug Deliv Sci Technol 75:103574. https://doi.org/10.1016/j.jddst.2022.103574

Publisher's Note